CHEMISTRY
A EUROPEAN JOURNAL

DOI: 10.1002/chem.200700479

How Can Rotaxanes Be Modified by Varying Functional Groups at the Axle?—A Combined Theoretical and Experimental Analysis of Thermochemistry and Electronic Effects

Christian Spickermann,[a] Thorsten Felder,[c] Christoph A. Schalley,*[b] and Barbara Kirchner*[a]

Abstract: We present theoretically as well as experimentally determined thermochemical data of the non-covalent interactions in different axle-substituted pseudorotaxanes. The overall interaction energy lies in the region of 35 kJ mol^{-1}, independent of the substitution pattern at the axle. Because rearrangement energies of 7 and 3 kJ mol^{-1} are required for wheel and axle, respectively, the sum of the net interactions of individual non-covalent bonds must exceed 10 kJ mol^{-1} to achieve a successful host–guest interaction. The geometrical analysis shows three hydrogen bonds, and the close inspection of the individual dipole moments as well as the individual hydrogen bonds reveals trends according to the different functional groups at the axle. The individual trends for the different hydrogen bonds almost lead to a cancellation of the substitution effects. From solvent-effect considerations it can be predicted that the pseudorotaxane is stable in $CHCl_3$ and CH_2Cl_2, whereas it would dethread in water. Comparing experimentally and theoretically calculated Gibbs free enthalpies, we find reasonable agreement if an exchange reaction of one solvent molecule instead of the direct formation reaction is considered.

Keywords: computer chemistry · density functional calculations · rotaxanes · supramolecular chemistry · thermochemistry

Introduction

The term "rotaxane" refers to a class of supramolecular complexes that consist of two mechanically linked components: the axle, a linear molecule with two sterically demanding functional groups at both ends (stoppers), and the wheel that surrounds the axle but is not connected with it in terms of a covalent bond.[1] Structures without appropriate stopper groups at the end of the axle are referred to as pseudorotaxanes. The rotaxane structure is seen as a possible basis for the realisation of a molecular motor, because the axle can deslip and is held inside the wheel's cavity merely by weak, non-covalent bonds.[2–5] The synthesis of a real rotaxane-based molecular motor has not yet been achieved at the microscopic level, although this is regarded as possible in principle, as nature gives a working example with the enzyme F_0F_1-ATP synthase.[2,3] This enzyme is capable of generating ATP from ADP and phosphate by conformational changes of an enzyme pocket induced by a unidirectional 120°-rotation of the axle-like F_1 component.[6,7] Concerning synthetic molecular motors on rotaxane basis, the unidirectional rotation could be introduced by topological chirality.[3,8] A more detailed overview of theoretical ap-

[a] Dipl.-Chem C. Spickermann, Prof. Dr. B. Kirchner
Theoretische Chemie
Wilhelm-Ostwald-Institut für Physikalische und Theoretische Chemie
Universität Leipzig
Linnestrasse 2, 04103 Leipzig (Germany)
Fax: (+49) 341-9736399

[b] Prof. Dr. C. A. Schalley
Organische Chemie, Institut für Chemie und Biochemie
Freie Universität Berlin
Takusstrasse 3, 14195 Berlin (Germany)
Fax: (+49) 30-838-554817

[c] Dipl.-Chem T. Felder[+]
Kekulé-Institut für Organische Chemie und Biochemie
Universität Bonn
Gerhard-Domagk-Strasse 1, 53121 Bonn (Germany)

[+] Present address:
Laboratory of Macromolecular and Organic Chemistry
Eindhoven University of Technology
P.O. Box 513, 5600 MB Eindhoven (The Netherlands)

Supporting information for this article is available on the WWW under http://www.chemistry.org or from the author.

proaches to supramolecular chemistry can be found in reference [9].

The examination of the co-conformational selectivity of two dibenzo-[24]crown-8 macrocycles to different ammonia binding sites in a [3]rotaxane by the AM1 method or the estimation of hydrogen-bond enthalpies in polymeric urethane rotaxanes in terms of a mean-field model are examples of semiempirical approaches to supramolecular rotaxane chemistry.[10,11] A detailed study of amide-type rotaxane formation based on the AM1 level of theory including comparisons with experimental data was published by Peyerimhoff et al. two years ago, in which special attention was paid to the non-covalent interactions governing the formation process.[12,13] These interactions were also studied by use of density functional theory (DFT) in small appropriate model systems ("rotaxane mimics"), and two of these model systems will also be covered in the present work.[14,15]. The influences of molecular guest properties as well as microsolvation in terms of the first solvation sphere on computed interaction enthalpies in ionic inclusion complexes were analysed in an earlier study and gave first hints of the importance of solvent effects in static supramolecular calculations.[16] Further theoretical examinations concern the movement of the macrocycle along the axle (shuttling) as a one-dimensional translation in a simplified double-minimum potential, the influence of the Kohn–Sham frontier orbitals of shuttle and axle upon conductivity and electron tunnelling along the rotaxane, as well as the dynamic simulation.[4,17–19]

Because rotaxane syntheses do not work efficiently, usually non-covalent template effects[20–24] are exploited in order to generate the appropriate axle–wheel geometry required for the threaded topology. Such template effects rely on metal complexation[5,25–27], π-donor–π-acceptor interactions[28–30] or hydrogen bonding involving cations, neutrals or anions.[1,13]

Here we focus on hydrogen-bond-mediated template effects involving the Hunter–Vögtle tetralactam macrocycle **1** (Figure 1) and axles that bear a secondary amide group. Several experimental studies reported binding constants for this host and some analogues.[31,32] Among these, one study[32] reported a remarkably pronounced substituent effect at the host on the binding constant of a suitable diamide guest. Replacing the isophthaloyl groups with 2,6-pyridine dicarboxylic acid amides substituted at C(4) with electron-withdrawing substituents significantly increased the binding constants, whereas they were rather small if electron-donating groups were attached in the same position. We were interested in determining whether similar effects could be found upon changing the electron density in secondary benzoylamide guests upon substitution of the benzoyl ring at C(4). To test this, the guests **2–6** (Figure 1) were investigated.

Theoretical studies predict that amide rotation within the macrocycle from an out- (carbonyl group pointing away from the cavity) to an in-conformation (C=O pointing towards the cavity) is not energy demanding at all.[12] Consequently, the macrocycle can exist in a 3-out–1-in conformation. On this basis, a secondary amide guest can form a maximum of three hydrogen bonds, because a fourth bond would lead to a structural distortion too large to be compensated by the hydrogen-bond energy. The guest N–H is able to form a third hydrogen bond with the carbonyl group of the macrocycle that is in the in-conformation. This is in line with the experimental fact that secondary amides are the only class of carbonyl compounds that bind to the macrocycle significantly, whereas ketones, acid chlorides and esters only bind very weakly.[31]

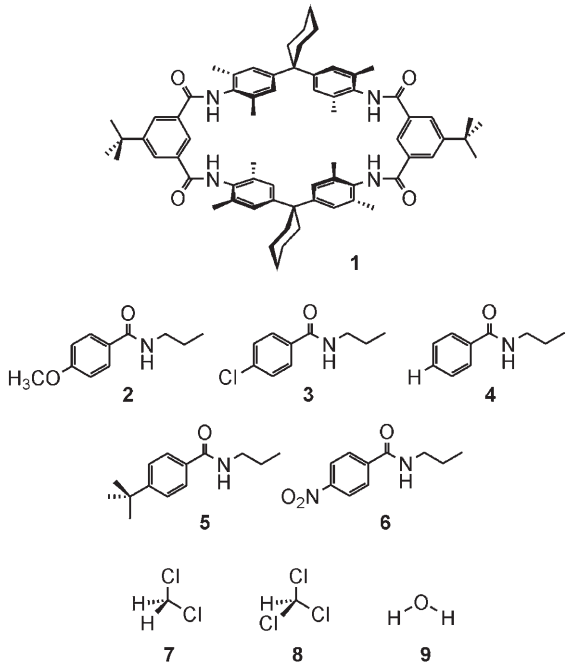

Figure 1. Chemical structure of the wheel and all axles investigated. **1**: wheel, **2**: MeO-axle, **3**: Cl-axle, **4**: H-axle, **5**: *t*Bu-axle, **6**: NO_2-axle, **7**: CH_2Cl_2, **8**: $CHCl_3$, **9**: H_2O, **10**: $(H_2O)_4$, **11**: $(CHCl_3)_2$.

In this contribution, theory and experiment are combined to provide a more detailed understanding of the effects mediating the binding of amides to macrocycle **1**. The investigated systems are introduced below, followed by the experimental and theoretical methodology. Afterwards, we present the results concerning structures, energetics, electronic properties, and thermodynamics, and compare the theoretical results to those obtained from experiment.

Systems investigated: All investigated pseudorotaxane complexes employ the same tetralactam macrocycle **1** as the wheel, but have different functional groups at one end of the axle (Figure 1). The central structural moiety of all axles **2–6** lies in the benzylamide group, which is able to act as a hydrogen-bond acceptor (through the carbonyl part) and a hydrogen-bond donor (through the N–H part) at the same time.[14,15]

The nitro group is a representative for a substituent with a strong electron-withdrawing mesomeric effect (–M), whereas chlorine exerts a strong electron-withdrawing inductive effect (–I). *tert*-Butyl with its moderate +I and

methoxy with a strong +M effect complete the series on the electron-donating side. From a simple point of view, one might expect hydrogen bonding to be strengthened for the methoxy-substituted benzoylamide, as shown in Figure 2. An increase in the electron density at the axle's carboxamide oxygen atom was expected to contribute to the formation of stronger hydrogen bonds. Similar arguments explain why electron-withdrawing groups should be expected to weaken the complex.

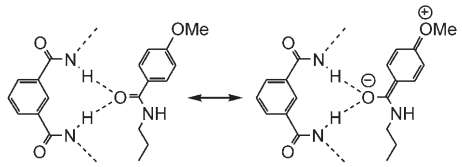

Figure 2. Mesomeric structures of the methoxysubstituted axle rationalise why stronger hydrogen bonds with the wheel should be expected.

Considering the comparison with experimental data, a series of additional complexes hosting a single dichloromethane molecule **7** and a single chloroform molecule **8** as the guest as well as the isolated macrocycle were also examined. These structures help to simulate the formation reaction of the pseudorotaxane complexes, as the synthesis and the NMR titration measurements are carried out in dichloromethane and chloroform solution, respectively. To gain further insight into possible solvent effects on the rotaxane formation, some additional calculations on complexes including one single water molecule **9**, a hydrogen-bonded chain of four water molecules **10**, and two chloroform molecules **11** as guests were also done. The thermochemical quantities of the two smaller systems **12** and **13** acting as hydrogen-bonded rotaxane mimics are also discussed below. These represent idealised models of the two-fold and one-fold hydrogen bond (Figure 3).[15]

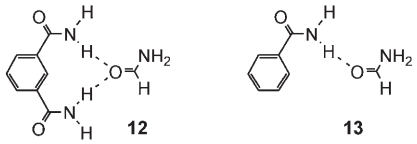

Figure 3. Rotaxane mimics as model systems of the two-fold and one-fold hydrogen bond.

Experimental Section

The macrocycle was synthesised by standard laboratory procedures.[33–35] The benzoyl amide guests were synthesised by simple amide coupling.[37–39] Before the binding constants can reliably be determined, it is mandatory to evaluate the complex stoichiometry that was established utilising ^{1}H NMR experiments with a Job's plot analysis in $CDCl_3$.[40,41] Maxima in all plots appeared at a molar fraction of 0.5 indicating the formation of 1:1 complexes. Because guest exchange is fast on the NMR timescale, binding constants were evaluated by ^{1}H NMR titrations in $CDCl_3$. Upon addition of the guest, all amide protons shift significantly due to the formation of hydrogen bonds. The titration curves were fitted by using a global least-squares fitting program (Spectrum Software Associates, Chapel Hill, NC, USA;[42] and literature cited therein) using the Levenberg–Marquardt method. Excellent fits were obtained with a model taking into account the free host, the free guest and the 1:1 complex. Only very slight improvements were found when 1:2 host–guest complexes were added to that model. However, the binding constants of the second guest were negligibly small ($<3\,\mathrm{M}^{-1}$) so that we refrain from analysing the data including them. The data is summarised in Table 1

Table 1. Free binding energies ΔG_1^{exp} of guests **2**–**6** to macrocycle **1** at $T=303$ K and $p=101\,325$ Pa. All values are in [kJ mol^{-1}].

Guest	No.	ΔG_1^{exp}
MeO-	**1**–**2**	−12.1
Cl-	**1**–**3**	−13.6
H-	**1**–**4**	−11.0
*t*Bu-	**1**–**5**	−11.4
NO_2-	**1**–**6**	−13.7

For complex **1**–**3**, the binding constants were determined depending on the temperature. Evaluation of the data through a van't Hoff plot of ln$K$ vs $1/T$ provided the binding enthalpy ($\Delta H^{exp}=-22.0$ kJ mol^{-1}) and binding entropy ($T\Delta S^{exp}=-8.8$ kJ mol^{-1}) of this host–guest pair. From this data, it becomes clear that host–guest binding is mainly driven by enthalpy and counterbalanced only by a small unfavourable entropy contribution. The negative entropy value indicates an entropy loss upon complex formation and thus is in line with the assumption that conformational degrees of freedom within the macrocycle are frozen out for a favourable binding geometry.

Theoretical Details

The structures of all compounds were optimised. Because of very large atom numbers (181 and more), density functional theory (DFT) combined with the resolution of identity technique (RI) was selected.[43] For the same reasons, the TZVP basis set in combination with the gradient-corrected functional BP86 was chosen.[44,45] In some cases second-order Møller–Plesset perturbation theory (MP2) calculations employing the TZVP or the TZVPP basis sets were carried out for the evaluation of the DFT results.[44] All calculations were performed using the TURBOMOLE 5.5 program package, and the obtained complex interaction energies were counterpoise-corrected by the procedure introduced by Boys and Bernardi.[46,47] The adiabatic complex interaction energies ΔE_{adia} can be calculated according to the supramolecular approach by subtracting the energies of the relaxed monomers E_{wheel}^{relax}, E_{guest}^{relax} as well as the BSSE contributions from the total cluster energy E^{tot}[48–51] [Eq. (1)]:

$$\Delta E_{adia} = E^{tot} - E_{wheel}^{relax} - E_{guest}^{relax} - \Delta E_{BSSE} \quad (1)$$

Considering the fact that the free compounds will undergo a conformational change upon complex formation and that the change of energy associated with this process does not directly contribute to the binding energy of the hydrogen bonds, an additional correction term to the interaction energy was calculated [Eq. (2)]:

$$\Delta E^{CF} = (E_{wheel}^{relax} - E_{wheel}^{unrelax}) + (E_{guest}^{relax} - E_{guest}^{unrelax}) \quad (2)$$

yielding the strained interaction energy ΔE_{strain}^{CP} (see Supporting Information). Furthermore, the computation of dipole moments and shared electron numbers (SEN) was carried out.[46] The determination of the two-centre SEN values and the computation of partial charges were based on the Davidson population analysis.[52,53] In the SEN approach the linear re-

lationship between the two-centre shared-electron number of a hydrogen bond and its binding energy allows an estimation of the bond strength if the parameters m and b of the corresponding linear equation [Eq. (3)] are known[54]:

$$E_{HA}^{\sigma} = m\sigma_{HA} + b \quad (3)$$

in which σ_{HA} denotes the two-centre SEN between the donor hydrogen atom H and the acceptor atom A, and b the axis intercept of the linear equation. This procedure has already been used for a broad variety of chemical applications concerning hydrogen bonding.[49,54–56]

The slope parameter m depends on the acceptor atom of the hydrogen bond and was determined for a wide range of hydrogen bonds involving large numbers of different atoms as reported in previous studies.[57] In the present application, the values $m = -724\ \mathrm{kJ\,mol^{-1}\,e^{-1}}$ and $b = 2.01\ \mathrm{kJ\,mol^{-1}}$ are chosen in agreement with amide-type hydrogen bonds and the BP86/TZVP combination.[58] Values for the total hydrogen-bond energy in terms of the SEN method are obtained by summing up the energies of all hydrogen bonds in the complex.

All frequency calculations were carried out by using the SNF program.[59] Thermochemical properties are derived from the canonical partition function at the standard p,T values of $p = 101\,325$ Pa and $T = 298.15$ K following standard textbook procedures for the ideal gas.[60] This means that even in calculations employing continuum solvation models such as COSMO, the translational and rotational entropy contributions for the gas phase are employed, which do not accurately reflect the conditions in the condensed phase due to solvent–solute interactions and a clearly reduced free volume of translation in the fluid.[61] Previous computational studies employed an approach suggested by Williams et al., which considers the transition to the fluid as a two-step process by first condensing the gaseous compound to a pure liquid and subsequently diluting the pure liquid to the 1 M standard state.[62–64] This procedure should, in principle, give more accurate results concerning entropy changes in solution and comparison with experimental data, but we refrain from using this approach because our aim is to predict entropy changes from pure theory. The method of Williams et al. requires knowledge of macroscopic quantities, for example, the condensation entropy, that are not available in the single-molecule picture.[64]

All enthalpies computed by the SNF program do not contain contributions from the electronic interaction energy and thus were corrected according to $\Delta_R H = \Delta H_{SNF} + \Delta E_{adia}^{CP}$ and $\Delta_R G = \Delta G_{SNF} + \Delta E_{adia}^{CP}$, respectively. The natural population analysis (NPA) was carried out by using the Gaussian 03 program package on the Hartree–Fock level of theory.[65] Because all examined systems exhibit large atom numbers, the basis set was decreased to 3-21G for the NPA calculations.[66,67]

Results

Structures: All investigated pseudorotaxanes form three hydrogen bonds, namely between the hydrogen atoms of two amide groups of the wheel and the oxygen atom of the axle's amide group and the a-w hydrogen bond (Figure 4, see Supporting Information for starting structures and the converged geometries).

Besides minor twisting in the propyl group of the axle and relaxation of the wheel, the basic structure of all complexes is preserved after the optimisations, that is, the local minimum structures on the potential surface still contain three hydrogen bonds in the case of the pseudorotaxane complexes. The minimum structures found for the compounds containing more than one solvent molecule as guests are depicted in Figure 5. The hydrogen-bonded water chain in the cavity of **1**–**10** is preserved during the optimisation, whereas

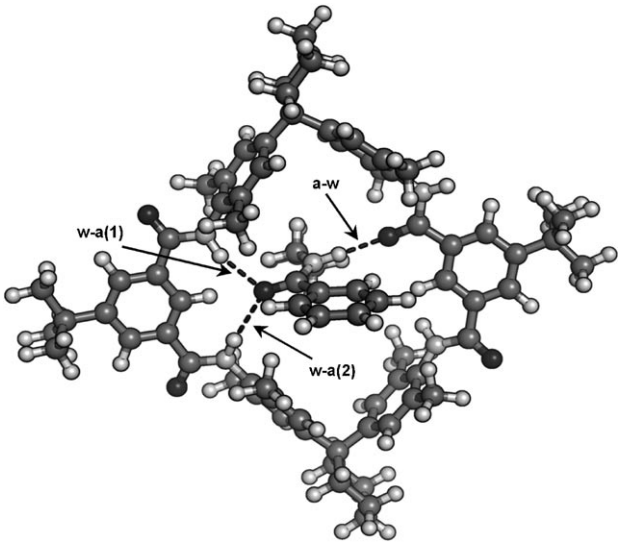

Figure 4. Starting conformation of rotaxane complexes shown exemplarily for complex **1**–**3**. Hydrogen bonds are marked.

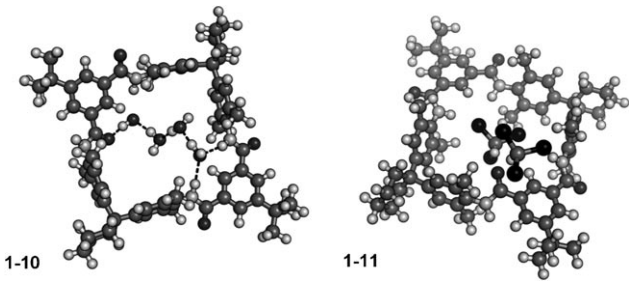

Figure 5. Minimum structures for the water-chain complex **1**–**10** and the dichloroform complex **1**–**11** (BP86/TZVP).

the second chloroform guest of **1**–**11** is driven out of the cavity and in the minimum structure rests over the plane spanned by the wheel and the first chloroform molecule.

The bond lengths as well as the bond angles between the nitrogen atom, hydrogen atom and oxygen atom are summarised in Table 2 (see Figure 4 for denotation of hydrogen bonds in pseudorotaxanes).

All values calculated for **1**–**2** to **1**–**6** are within roughly the same range. The N–O distances follow the trend of the hydrogen-bond lengths in most cases, thus resulting in nearly undisturbed N–H bond lengths of ~99 pm on average. This is also true for the water-chain complex **1**–**10**. Compared to the N–H bond lengths obtained for isolated **1** (~102 pm), this is only a slight decrease, but corresponds well to the change in bond length in rotaxane mimics.[15] Compound **1**–**8** ($CHCl_3$) shows a guest-to-wheel hydrogen bond that agrees well with the values of the pseudorotaxane complexes, whereas the hydrogen bond in **1**–**7** (CH_2Cl_2) is somewhat elongated. The smallest distances are found for the structures involving water molecule guests and $OH_{guest} \rightarrow O_{wheel}$ hydrogen bonds, with **1**–**10** ($(H_2O)_4$) showing the shortest bond of all investigated compounds. This significantly re-

Table 2. Bond lengths r_1(H···O), r_2(N···O) and bond angles α(N-H···O) of all three hydrogen bonds for complexes **1–2** to **1–6** as well as the corresponding values for the CH···O hydrogen bonds found for complexes **1–7**, **1–8** and **1–11** and the OH···O hydrogen bonds in **1–9** and **1–10**. In the case of multiple bonds in **1–10** and **1–11** the shortest bond of each connectivity is given. Abbreviations: w = wheel; a = axle (guest).

		w→a(1)			w→a(2)			a→w		
Guest	No.	r_1 [pm]	r_2 [pm]	α [°]	r_1 [pm]	r_2 [pm]	α [°]	r_1 [pm]	r_2 [pm]	α [°]
					axle–wheel complexes					
MeO-	**1–2**	213	312	162.0	239	338	164.5	208	306	160.5
Cl-	**1–3**	215	314	163.6	242	341	160.7	204	303	162.2
H-	**1–4**	215	314	164.1	241	340	161.2	206	304	159.4
*t*Bu-	**1–5**	215	314	164.2	239	339	161.6	207	304	159.8
NO_2-	**1–6**	218	316	163.2	244	344	159.6	202	301	162.0
					solvent complexes					
CH_2Cl_2	**1–7**	–	–	–	–	–	–	215	324	175.1
$CHCl_3$	**1–8**	–	–	–	–	–	–	202	311	172.2
H_2O	**1–9**	–	–	–	–	–	–	199	294	160.6
$(H_2O)_4$	**1–10**	207	307	163.2	246	346	165.6	171	270	166.8
$(CHCl_3)_2$	**1–11**	–	–	–	–	–	–	205	313	163.8

duced distance, especially relative to **1–9** (H_2O), hints at additional steric influences, which seems reasonable for the water-chain complex **1–10** fitting well into the confined space provided by the wheel **1**.

Comparison of the angles found for the two short bonds (w→a(1), a→w) and the elongated bond (w→a(2)) shows that these values fall within a narrow range of 159 to 165°. Thus, all three hydrogen bonds in **1–2** to **1–6** are regulated solely by their interatomic distances that vary between 202 and 244 pm, whereas all predicted angles have very similar values of around 160°.

To examine the influence of hydrogen-bond formation on the geometry of the macrocycle, we determined the square dimension of the area between all four nitrogen atoms in the wheel and compared the results to the corresponding values of structures **1–7** to **1–10** and the free wheel **1**. This data is given in the Supporting Information. Assuming that the guest is large enough to form more than one hydrogen-bond contact, it is expected that this area is reduced upon hydrogen-bond formation and that the extent of the reduction is correlated to the degree of interaction between host and guest. In the cases of **1–2** to **1–6**, the area within the macrocycle is significantly reduced relative to **1** and **1–8** ($CHCl_3$). Complex **1–6**(NO_2-) shows the smallest area reduction, however, this is still about ~5000 pm^2 lower than the free macrocycle. The dichloromethane complex **1–7** is affected in a significant way as well. In the case of the chloroform compound **1–8**, almost no area reduction is observable. The largest reduction is found for **1–2** (MeO-) and **1–5** (*t*Bu-). Because the water guest is a very small molecule capable of establishing relatively strong hydrogen bonds, the calculated area reduction for **1–9** (H_2O) is not directly comparable to the other values. Due to the flexible behaviour of the four-membered water chain, this decreased effect on the cavity of the host **1** is also observable for compound **1–10** ($(H_2O)_4$). One should keep in mind that the calculated area reduction is no direct evidence for hydrogen-bond formation, but merely hints at such interactions through an induced conformational change of the macrocycle.

Energetics: The interaction energies are summarised in Table 3. It is apparent that both interaction energies ΔE^{CP}_{adia} and ΔE^{CP}_{strain} remain within narrow ranges for all five pseudorotaxanes. Thus, a discussion of electronic substitution influences is not necessary. Compound **1–6** (NO_2-) shows the smallest absolute adiabatic interaction energy as well as the weakest strained interaction energy of all pseudorotaxanes, indicating the electron-withdrawing effect of the *p*-nitrophenyl group at the end of the axle. In the case of **1–7** (CH_2Cl_2), the obtained interaction energies roughly equal one third of the pseudorotaxane interaction energies, which agrees with the observation of one or two rather weak hydrogen bonds, see above. In contrast to this, the calculated interaction energies for the chloroform complex **1–8** are significant lower and only equal one half of the values obtained for **1–7**, although both structures exhibit the same number and kind of hydrogen bonds. A slightly increased value of -8.8 kJ mol^{-1} is predicted for the dichloroform complex **1–11**. Both complexes containing water as guest show an increased interaction energy compared to the expected number of hydrogen bonds. Considering the four OH···O hydrogen bonds in **1–10** ($(H_2O)_4$), the calculated in-

Table 3. BSSE, interaction energies ΔE^{CP}_{adia} and strained energies ΔE^{CP}_{strain}. ΔE^{CF}_{wheel} denotes the contribution to ΔE_{strain} arising from the wheel; ΔE^{CF}_{guest} gives the corresponding value for the guest (in cases **1–10** and **1–11** the mean values per guest molecule are given). The column ΔE^{CP}_{Cosmo} corresponds to interaction energies obtained from COSMO calculations ($\varepsilon = 4.81$).[61] All values in [kJ mol^{-1}].

Guest	No.	BSSE	ΔE^{CP}_{adia}	ΔE^{CP}_{strain}	ΔE^{CF}_{wheel}	ΔE^{CF}_{guest}	ΔE^{CP}_{Cosmo}
				axle–wheel complexes			
MeO-	**1–2**	−6.4	−37.9	−48.4	−7.5	−3.3	−0.5
Cl-	**1–3**	−6.2	−36.6	−47.2	−7.4	−3.2	0.4
H-	**1–4**	−6.2	−36.5	−46.9	−7.3	−3.1	0.6
*t*Bu-	**1–5**	−6.2	−36.0	−46.8	−7.3	−3.5	1.9
NO_2-	**1–6**	−6.2	−35.7	−46.6	−7.5	−3.4	2.2
				solvent complexes			
CH_2Cl_2	**1–7**	−4.2	−13.9	−16.3	−1.8	−0.6	–
$CHCl_3$	**1–8**	−4.4	−6.8	−8.4	−1.1	−0.5	8.7
H_2O	**1–9**	−5.1	−23.2	−25.5	−2.0	−0.3	–
$(H_2O)_4$	**1–10**	−19.2	−65.2	−107.5	−10.8	−7.5	–
$(CHCl_3)_2$	**1–11**	−7.8	−8.8	−12.8	−3.5	−0.2	–

teraction energies are quite large compared to the pseudorotaxanes and the single water complex **1–9**.

The contributions to the strained interaction energy are very similar as well, predicting a rearrangement energy of ~10 kJ mol^{-1} for structures **1–2** to **1–6**. Thus, to form a rotaxane of the structural motif encountered in **1–2** to **1–6**, an approximate rearrangement energy of ~10 kJ mol^{-1} has to be provided. With respect to this point, the wheel is affected more significantly, showing values around ~7 kJ mol^{-1}. Again, the influence of the substitution pattern is not clearly visible. As could be expected, the contributions to ΔE^{CP}_{strain} in the case of **1–7** (CH_2Cl_2), **1–8** ($CHCl_3$), **1–9** (H_2O) and **1–11** (($CHCl_3)_2$) are much smaller due to the weaker complex interactions and the smaller number of hydrogen bonds found for these structures. The influence of the water chain in **1–10** (($H_2O)_4$) is again clearly visible in enlarged values especially for the wheel rearrangement.

A plot between the calculated interaction energies and the experimental free binding enthalpies is illustrated in Figure 6. In the case of compounds **1–3** to **1–6**, the linear correlation is somewhat well obtained, whereas **1–2** can be identified as the largest outlier even if the experimental error of ~2 kJ mol^{-1} in ΔG_1^{exp} is considered.

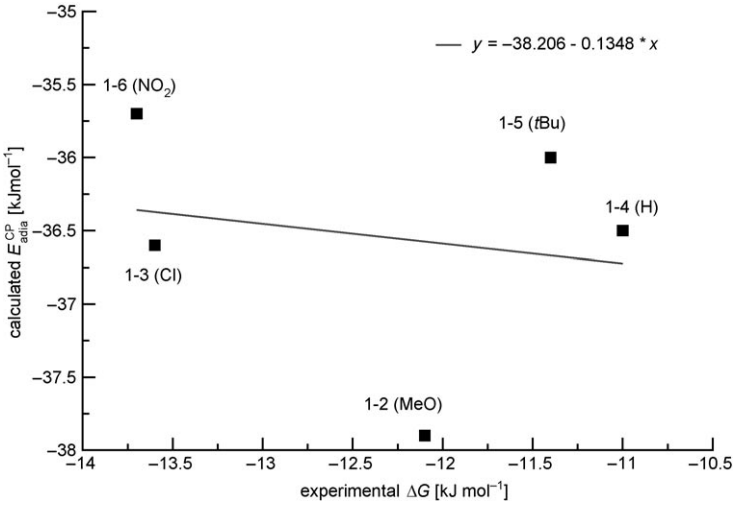

Figure 6. Calculated adiabatic interaction energy ΔE^{CP}_{adia} plotted against the experimental free binding enthalpy ΔG_1^{exp}.

To examine the accuracy of the DFT-computed interaction energy with respect to this observation, additional BP86 and MP2 calculations were performed for the truncated systems given in Figure 2, which illustrates the mesomeric forms (the axle propyl group was furthermore replaced by a methyl group and the wheel fragment amide nitrogen atoms were saturated with hydrogen atoms). The results of these computations are summarised in Table 4.

These numbers demonstrate that the influence of the axle substitution is quite well captured by DFT in the case of the methoxy and the chlorine substituents, whereas in the case of the remaining substituents both methods predict a difference in interaction energy of ~10 kJ mol^{-1}. The large differences to the interaction energies ΔE^{CP}_{adia} listed in Table 3 are due to the restriction to the two-fold hydrogen bridge w→a(1,2), which is the only hydrogen-bond connection considered in this model calculation. The special behaviour of the **2** (MeO-) pseudorotaxane could thus be rooted in the bad description of dispersion for the other complexes.

Table 4. Adiabatic interaction energies ΔE^{CP}_{adia} for truncated complexes (see Figure 2 and text) obtained from BP86 optimisations and MP2 single-point calculations. The TZVP basis set was used throughout. All values in [kJ mol^{-1}].

		BP86		MP2	
Guest	No.	BSSE	ΔE^{CP}_{adia}	BSSE	ΔE^{CP}_{adia}
MeO-	**2**	−1.9	−40.0	−12.1	−41.0
Cl-	**3**	−2.7	−33.0	−12.1	−36.9
H-	**4**	−2.7	−18.1	−11.3	−27.7
*t*Bu-	**5**	−2.8	−19.4	−11.8	−28.5
NO_2-	**6**	−2.5	−9.7	−10.5	−20.2

Another reason for the outlying behaviour of complex **1–2** could lie in the specific position of the methoxy group, which in principle can freely rotate around the C–O bond. To check this possibility, several structure optimisations were carried out for different dihedral angles C-C-O-Me, which without exception converged to the flat arrangement with an dihedral angle of ~0°. In addition, two constrained optimisations were performed by fixing the dihedral angle to values of 45 and 90°, respectively. The results for the geometries obtained from these calculations proved that such constrained structures are about 97 kJ mol^{-1} (45°) and 105 kJ mol^{-1} (90°) higher in energy than the corresponding relaxed geometries. Obviously, the interaction between the π system and the lone pairs of the oxygen atom in the methoxy group receives a maximal stabilisation at a dihedral angle of ~0°.

Above, we suggested the idea of taking a structural parameter, for example, the square area within the macrocycle, as a measure for the interaction strength between wheel and guest. Compared to the calculated adiabatic interaction energies, the trend of area reduction is roughly reproduced, at least considering the weakest- and strongest-bound pseudorotaxanes **1–6**, **1–2** as well as the dichloromethane complex **1–7** and the chloroform complex **1–8** (see Supporting Information). In the case of structures **1–3** (Cl-), **1–4** (H-), **1–5** (*t*Bu) and the water-containing structures **1–9** (H_2O) and **1–10** (($H_2O)_4$), the correlation between area reduction and interaction energy is clearly absent, which again might be a result of the error-proneness due to the similar values obtained for these structures and additional steric effects of the water chain in the case of **1–10**.

Wave-function analysis: For a summary of the electronic properties of all investigated structures see Tables 5 and 6. Please note that the dipole moment of the isolated wheel amounts to 5.65 D. The computed total dipole moments μ_{tot} for the pseudorotaxanes as well as **1–10** (($H_2O)_4$) are within a narrow range of 11–12 Debye, whereas the other solvent

Table 5. Computed dipole moments μ. All values are in [D] (β [°] denotes the angle between the dipole moment of host and guest in the complex geometry). $\mu^{MP2,axle}$ contains additional MP2/TZVPP values. In the case of **1–11**, the axle values in the complex geometry are mean values per guest molecule.

		isolated		complex			
Guest	No.	μ_{axle}	μ_{axle}^{MP2}	μ_{wheel}	μ_{axle}	μ_{tot}	β
			axle–wheel complexes				
MeO-	**2**	2.52	3.23	5.72	2.98	11.40	27.8
Cl-	**3**	3.50	3.47	5.75	3.74	11.34	52.4
H-	**4**	3.49	3.80	5.73	3.66	11.78	33.9
*t*Bu-	**5**	3.66	4.08	5.74	3.83	12.04	30.7
NO_2-	**6**	5.51	5.33	5.78	5.74	11.11	80.8
			solvent complexes				
CH_2Cl_2	**7**	1.80	1.86	5.70	1.83	8.42	24.3
$CHCl_3$	**8**	1.18	1.24	5.67	1.21	8.02	15.8
H_2O	**9**	2.13	2.06	5.73	2.15	7.63	13.5
$(H_2O)_4$	**10**	3.81	3.45	5.30	7.62	11.35	31.2
$(CHCl_3)_2$	**11**	1.18	1.24	5.47	1.20	7.86	16.6

Table 6. Results of the NPA for complexes **1–2** to **1–6**. Values for the charge analysis refer to the hydrogen atom (q^{don}) and hydrogen-bond acceptor (q^{acc}). For denotation of hydrogen bonds, see Table 2. All charges are in [e].

		w→a(1)		w→a(2)		a→w	
Guest	No.	q^{don}	q^{acc}	q^{don}	q^{acc}	q^{don}	q^{acc}
MeO-	**1–2**	0.454	−0.765	0.449	−0.765	0.457	−0.703
Cl-	**1–3**	0.452	−0.755	0.447	−0.755	0.460	−0.707
H-	**1–4**	0.453	−0.758	0.448	−0.758	0.459	−0.703
*t*Bu-	**1–5**	0.453	−0.761	0.449	−0.761	0.458	−0.701
NO_2-	**1–6**	0.450	−0.747	0.445	−0.747	0.463	−0.712

complexes show a reduced total dipole moment of about 8 Debye. Axle **6** (NO_2-) assumes the largest value of all guests in both isolated and complex geometry and comes close to the corresponding value obtained for the free macrocycle **1** (5.65 D), whereas the total dipole moment computed for pseudorotaxane **1–6** (NO_2-) is smaller than that of all other complexes (with the exception of most of the solvent complexes). Axle **2** (MeO-) shows the smallest result of all pseudorotaxane components in both geometries, lying only 0.39 Debye (0.83 Debye for the strained geometry) above the water guest. These results thus yield the unexpected observation that the axles with the smallest isolated dipole moment belong to complexes with the largest interaction energy and vice versa (compare Table 3), which means that the acceptor function of the axle is dominant.

We find a slight increase in the dipole moments of all components by comparing isolated to complex geometries, that is, the complex formation leads to a polarisation of all structures with the exception of the macrocycle **1** in the multiple complexes **1–10** ($(H_2O)_4$) and **1–11** ($(CHCl_3)_2$). In these cases the wheel (5.30 and 5.47 D, respectively) is depolarised, that is, its dipole is smaller than the value of the isolated **1** (5.65 D). The trend of increasing dipole moments as interaction energy decreases observed for the axles in the isolated geometry is also true for the strained geometries, with the exception of axles **3** (Cl-) and **4** (H-), which show an inverted order of values.

The angles β computed for **1–2** to **1–6** predict a rather flat arrangement of the dipole moments. However, the optimal arrangement seems not to be possible due to the structural constraints induced by the hydrogen bonds (see Figure S2 in the Supporting Information). Altogether, the computed values are rather large compared to, for example, water (2.13 D) and compound **1–9** (7.63 D), which indicates that dipole–dipole interactions must play a non-negligible role in the overall host–guest interaction, as discussed elsewhere for different functional groups.[68]

As already noted, a comparison between the dipole moments of the axles **2** (MeO-) to **6** (NO_2-) in the isolated geometry and the interaction energies listed in Table 3 indicates a direct connection of increasing interaction energy and decreasing dipole moment, that is, the weakest-bound complex **1–6** (NO_2-) corresponds to the isolated guest with largest dipole moment, and the strongest-bound complex **1–2** (MeO-) corresponds with the smallest isolated axle dipole. This inverse relation is even more obvious for the more accurate MP2/TZVPP results shown in Table 5 and corresponds to the correlation of molecular-guest properties with host–guest interaction energies, as already observed for smaller inclusion complexes.[16] The most strongly bound pseudorotaxane **1–2** (MeO-) not only exhibits the smallest total dipole moment, but also the smallest dipole angle. This indeed might be interpreted as a combined hydrogen-bond and dipole–dipole contribution to the interaction energy or as a more easily achievable rearrangement to the ideal dipole–dipole position for complexes with less-rigid hydrogen bonds. Figure 7 illustrates the calculated dipole moment for isolated axles **2** (MeO-) to **6** (NO_2-) plotted against the experimental free binding enthalpy of the corresponding complexes **1–2** to **1–6**. In this plot compounds **1–2** and **1–6** can be identified as outliers if a linear relation between axle dipole moment and experimental ΔG_1^{exp} values is assumed, whereas **1–3** to **1–5** are somewhat better fitting. The MP2/TZVPP result for **1–2** (MeO-) turns out to be more consistent with respect to the remaining data points as well, but still yields a rather small value.

As mentioned above, the reason for the exceptional behaviour of **1–6** in Figure 7 and of **1–2** (MeO-) in Figures 7 and 6 cannot be solely attributed to the fact that additional interactions possibly important for the host–guest interaction are poorly treated by DFT. The results from Tables 4 and 5 and Figures 6 and 7 rather indicate an especially strong treatment of the stabilising substitution effect in **1–2**

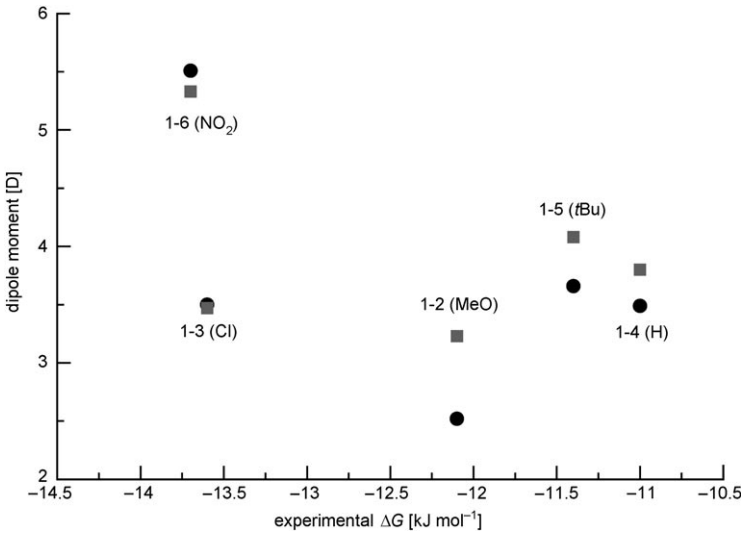

Figure 7. Calculated dipole moments (●: BP86, ■: MP2) for axles **2** to **6** plotted against the experimental free binding enthalpy ΔG_1^{exp}.

(MeO-) by DFT relative to the other complexes and a corresponding reverse effect in **1–6**. Furthermore, a contribution to the interaction energy not considered so far is expected to result in a less-stable bound complex, that is, the outliers should occur in the more positive region of Figure 6. This is not the case for compound **1–2**.

To compare charges on the hydrogen atoms and hydrogen-bond acceptors we performed a natural population analysis (NPA) on the equilibrium geometries of all pseudorotaxanes as introduced by Weinhold et al. (see Table 6).[69]

The values obtained for all three hydrogen bonds are very similar. The only significant difference can be found for the a→w oxygen-acceptor atom, which lies ~0.05 e above the computed values of the two other hydrogen-bond acceptors, and the w→a(2) hydrogen atom, which shows a slightly reduced charge relative to the other hydrogen atoms involved in hydrogen bonding. This is in accordance with the results described above, in which the w→a(2) bond was predicted to be longer than the w→a(1) bond by ~25 pm.

The two-centre shared-electron numbers (SEN) calculated for all atoms involved in hydrogen bonding are summarised in Table 7. In all cases, the largest SEN is associated with either the wheel-to-axle hydrogen bond w→a(1) or the single axle-to-wheel hydrogen bond a→w. This fact is in accord with the bond lengths from Table 2, in which these hydrogen bonds are the ones with the shortest interatomic distances. The SEN of the wheel-to-axle hydrogen bond w→a(2) is less than half of that found for the other two bonds (e.g., 0.0089 e compared to 0.0226 e and 0.0232 e, respectively, for compound **1–3**), which indicates only a minor contribution from this bond to the overall interaction energy of the complex.

The results of the SEN method for the estimation of hydrogen-bond strengths applied to complexes **1–2** to **1–6** are also summarised in Table 7.

As expected, the overall energies determined by the SEN method E_{total}^{σ} are smaller than the corresponding adiabatic interaction energies obtained from the supramolecular approach, ΔE_{adia}^{CP}. These results clearly demonstrate that the major contribution to the overall interaction energy obtained with BP86/TZVP is given by the binding energy of the hydrogen bonds, but further interactions seem reasonable.

The single hydrogen bonds lie within similar ranges for all five pseudorotaxanes, covering values ranging from −13.0 to −16.0 kJ mol^{-1} for the strong hydrogen bonds w→a(1) and a→w, whereas the weaker hydrogen bond w→a(2) assumes values of between −3.8 and −5.2 kJ mol^{-1}. Complex **1–2** (MeO-) is again predicted to form the strongest bonds.

The main observation from the individual hydrogen-bond energy analysis can be summarised by the following considerations: It is clear from Table 7 that only a small or almost no substitution trend in the energies (ΔE_{adia}^{CP} to ΔG_1^{exp}) can be observed. The substitution pattern provides opposite electronic trends, such that the donating and accepting group annihilate or blur these effects in an overall sense. For example, the methoxy group in **1–2** is supposed to weaken a donating hydrogen bond (see first line in Table 7, −13.1 compared to −13.9 kJ mol^{-1} for the unsubstituted structure **1–4** (H-)). At the same time it enhances the hydrogen-accepting bond w→a(1,2) (compare −15.8 kJ mol^{-1} predicted for **1–2** (MeO-) to −14.4 kJ mol^{-1} found for the unsubstituted case **1–4** (H-), see also Figure 2). This behaviour is inverted in the case of the NO_2 group, that is, the donor hydrogen bond is amplified (−16.0 to −13.9 kJ mol^{-1} in **1–4** (H-)) and the acceptor bonds are weakened (−13.0 to −14.4 kJ mol^{-1} in **1–4** (H-)). As the overall trend predicts a most stable **1–2** (MeO-) followed by **1–3** (Cl-) etc., the dominating hydrogen bond can clearly be identified to be the accepting bond for the axles, which was already indicated through the discussion of the dipole moments. This is surprising as one might expect that the substitution effect influences the donating group in a more significant way.

Table 7. Hydrogen-bond energies E_{HA}^{σ} and interaction energies ΔE_{adia}^{CP}. E_{total}^{σ} denotes the sum of the individual hydrogen-bond contributions E_{HA}^{σ} for a given complex. σ_{HA} in [e], energies in [kJ mol^{-1}].

		w→a(1)		w→a(2)		a→w			
Guest	No.	σ_{HA}	E_{HA}^{σ}	σ_{HA}	E_{HA}^{σ}	σ_{HA}	E_{HA}^{σ}	E_{total}^{σ}	ΔE_{adia}^{CP}
MeO-	**1–2**	0.0246	−15.8	0.0099	−5.2	0.0209	−13.1	−34.1	−37.9
Cl-	**1–3**	0.0226	−14.4	0.0089	−4.4	0.0232	−14.8	−33.6	−36.6
H-	**1–4**	0.0227	−14.4	0.0091	−4.6	0.0220	−13.9	−32.9	−36.5
*t*Bu-	**1–5**	0.0227	−14.4	0.0097	−5.0	0.0213	−13.4	−32.8	−36.0
NO_2-	**1–6**	0.0208	−13.0	0.0080	−3.8	0.0249	−16.0	−32.8	−35.7

Thermochemical properties: Now we focus on the comparison between experimental and computational free binding enthalpies. We obtain the computed free enthalpies firstly by the complex formation according to the reaction between the constituting monomers [Eq. (4)]:

$$\text{wheel} + \text{axle} \rightarrow \text{pseudorotaxane} \quad (4)$$

and secondly by an exchange reaction according to Equation (5):

$$\text{wheel} \cdot \text{solv} + \text{axle} \rightarrow \text{pseudorotaxane} + \text{solv} \quad (5)$$

Here the term "solv" abbreviates any kind of solvent molecule that serves as a guest at reaction start.

Furthermore, a combination of the interaction energies ΔE^{CP}_{Cosmo} obtained from the COSMO calculations and the free reaction enthalpies $\Delta_R G$ of the standard calculations is included in Table 8. Because the experimental measurements are carried out in chloroform, structure **1–8** ($CHCl_3$) together with the different axles **2** to **6** were used as reactants for the exchange approach concerning the comparison with the experiment, however, a summary of thermochemical properties employing the other solvent complexes is given as well. Because the interaction energy calculated for **1–8** ($CHCl_3$) is very similar to the one obtained for **1–11** ($(CHCl_3)_2$) (see Table 3), we expect no large difference in the thermochemical data upon reactant exchange from **1–8** to **1–11**. In addition, the thermochemistry of the two more-simple model systems **12** and **13** is presented as a sample case of more-flexible rotaxane mimics.[15] Table 8 summarises the results of the thermochemical analysis.

Table 8. Thermochemical quantities at $T = 298.15$ K and $p = 101\,325$ Pa. Complex **1–8** ($CHCl_3$) was used as reaction partner for all other guests in the case of the exchange reaction. $\Delta_R G_{Cosmo}$ denotes free reaction enthalpies based on the interaction energies ΔE^{CP}_{Cosmo} obtained from COSMO calculations ($\varepsilon = 4.81$). All values in [kJ mol^{-1}].

		formation				exchange			
Guest	No.	$\Delta_R H^f$	$T\Delta_R S^f$	$\Delta_R G^f$	$\Delta_R G^f_{Cosmo}$	$\Delta_R H^{ex}$	$T\Delta_R S^{ex}$	$\Delta_R G^{ex}$	$\Delta_R G^{ex}_{Cosmo}$
				axle–wheel complexes					
MeO-	**1–2**	−29.7	−49.0	19.3	56.7	−29.9	−2.3	−27.6	−5.5
Cl-	**1–3**	−28.1	−50.6	22.4	59.4	−28.3	−3.8	−24.5	−3.0
H-	**1–4**	−28.2	−50.4	22.2	59.3	−28.4	−3.7	−24.7	−3.1
*t*Bu-	**1–5**	−28.2	−49.5	21.3	59.2	−28.4	−2.7	−25.7	−3.3
NO_2-	**1–6**	−26.9	−52.1	25.1	63.0	−27.1	−5.3	−21.8	0.6
				solvent complexes					
CH_2Cl_2	**1–7**	−6.1	−41.5	35.5	–	−6.3	5.2	−11.5	–
$CHCl_3$	**1–8**	0.2	−46.7	46.9	62.4	0.0	0.0	0.0	0.0
H_2O	**1–9**	−14.4	−33.7	19.3	–	−14.6	13.1	−27.7	–
$(H_2O)_4$	**1–10**	−56.3	−52.7	−3.6	–	−56.5	−6.0	−50.5	–
				rotaxane mimics					
H(2-fold)	**12**	−29.0	−45.7	16.7	–	–	–	–	–
H(1-fold)	**13**	−16.0	−43.9	27.9	–	–	–	–	–

It is apparent that for all cases both proposed reaction types lead to contrary results concerning the free reaction enthalpy, and it is clear that this discrepancy arises from differences in the reaction entropy predicted for both pathways. A comparison of the reaction enthalpies $\Delta_R H$ shows that these values only differ at the first decimal place and systematically follow the same trend. Furthermore, the $\Delta_R H$ values predict an exothermic reaction in both cases. Moving on to the reaction entropy contribution $T\Delta_R S$, one immediately notices a large difference in the computed $T\Delta_R S$ values of about 35–40 kJ mol^{-1} between both reaction pathways. In the case of the exchange reaction, the computed absolute reaction entropy $\Delta_R S$ is much smaller (even positive for the solvent-exchange reactions **1–8** ($CHCl_3$)→**1–7** (CH_2Cl_2) and **1–8** ($CHCl_3$)→**1–9** (H_2O)) and the free reaction enthalpy $\Delta_R G$ is negative for all examined complexes, thus predicting thermodynamically stable pseudorotaxane structures. Because the entropy differences of all non-solvent exchange reactions are negative, we expect a formal decrease in entropy and more highly ordered reaction products for both suggested reaction pathways, which in the case of the reaction shown in Equation (5) can be compensated by the exothermic change in enthalpy and the release of the solvent guest. This confirms the idea of a template working as an entropic sink.

The computed $\Delta_R G^f$ values for **1–7** (CH_2Cl_2) to **1–9** (H_2O) are positive and even larger than all pseudorotaxane values (with the exception of **1–9**). For compound **1–10** ($(H_2O)_4$) we find a strongly exothermic reaction enthalpy, which should mainly be rooted in the formation of the additional host–guest hydrogen bonds, whereas the entropy term is only slightly affected. In the case of the rotaxane mimics **12** and **13**, the computed reaction enthalpies correspond well to the values obtained for **1–2** to **1–6**. The entropy values are again very large and predict endergonic formation reactions.

The mixed $\Delta_R G_{Cosmo}$ values reproduce the original $\Delta_R G$ trend quite well, but they are at the same time larger by about 35 kJ mol^{-1} in the case of the formation mechanism and by about 22 kJ mol^{-1} in the case of the exchange reaction.

To study the effect of different solvents on the exchange reaction according to Equation (5), the solvent complexes **1–7** to **1–10** were taken as reaction partners for the axles **2** to **6** instead of **1–8** (see Supporting Information). The results of these calculations demonstrate that the choice of the solvent guest has a strong influence upon the thermochemical reaction data, as could be expected from chemical intuition. This behaviour is not surprising concerning the large ΔE^{CP}_{adia} values obtained for **1–9** and **1–10**, which work as a drawback for the exchange towards the pseudorotaxane complexes due to the displacement that has to take place in the exchange mechanism. This indicates that even a small aqueous impurity in the solvent could hinder the rotaxane synthesis significantly.

After selecting the exchange-reaction mechanism [Eq. (5)] as the more probable variant of the pseudorotaxane formation, the computed thermochemical properties as

well as the thermally uncorrected interaction energies are now compared to the experimental free reaction enthalpies obtained from NMR-titration and the van't Hoff method (see above and Table 9).

Table 9. Calculated electronic and thermochemical energies of the exchange reaction [Eq. (5)] at $T=298.15$ K and $p=101\,325$ Pa compared to the experimental free binding enthalpies ΔG_1^{exp} at $T=303$ K. The chloroform complex **1–8** is chosen as reaction partner for all axles. ΔE_{adia}^{ZPE} corresponds to the adiabatic interaction energy corrected for the zero-point energy (ZPE). All values in [kJ mol^{-1}].

Guest	No.	ΔE_{adia}^{CP}	ΔE_{strain}^{CP}	ΔE_{adia}^{ZPE}	$\Delta_R H$	$T\Delta_R S$	$\Delta_R G$	$\Delta_R G_{Cosmo}$	ΔG_1^{exp}
MeO-	**1–2**	−37.9	−48.4	−35.8	−29.9	−2.3	−27.6	−5.5	−12.1
Cl-	**1–3**	−36.6	−47.2	−33.9	−28.3	−3.8	−24.5	−3.0	−13.6
H-	**1–4**	−36.5	−46.9	−33.9	−28.4	−3.7	−24.7	−3.1	−11.0
*t*Bu-	**1–5**	−36.0	−46.8	−34.6	−28.4	−2.7	−25.7	−3.3	−11.4
NO_2-	**1–6**	−35.7	−46.6	−32.6	−27.1	−5.3	−21.8	0.6	−13.7

Considering the computed $\Delta_R G$ results, we find a deviation of 10–15 kJ mol^{-1} for all cases between theory and experiment. The largest difference of about ~15 kJ mol^{-1} can again be observed for **1–2** (MeO-), which is no surprise, as already discussed above.

The differences between experimental results and the $\Delta_R G_{Cosmo}$ values are comparable, but in this case the reaction towards the pseudorotaxanes is predicted to be thermodynamically less favourable. For one single complex (**1–3**, Cl-), the experimental enthalpic and entropic contributions to the Gibbs free reaction enthalpy were determined by using the van't Hoff method, yielding values of $\Delta H^{exp}=-22.0$ kJ mol^{-1} and $T\Delta S^{exp}=-8.8$ kJ mol^{-1}, respectively. Again these numbers are in acceptable accordance with the theoretical values (see Table 9).

The overall results thus indicate that the dominating solvent effect concerning complex formation lies in the cavity occupation of the solvent particle, that is, the chloroform molecule from within the wheel. A closer agreement between static first principles calculation and experiment seems hardly achievable, as the dynamic character of the host–guest exchange is not included in this static model and our microsolvation approach is limited to a single solvent molecule in this case. Problems of this kind were also encountered in previous studies, but they might be reduced by a chemically sensible inclusion of additional solvent molecules within the cavity of the host.[63] The general importance of dynamic effects in supramolecular chemistry could also be shown previously by several molecular dynamic studies.[9,36,70,71] However, our results demonstrate the importance of actually including one solvent molecule in the cavity compared to the completely isolated gas-phase calculation, which yields values totally incomparable to the experimental data.

For the theoretical investigation of supramolecular systems in solution we thus suggest to examine reactions of the exchange type [Eq. (5)] instead of the simple direct formation according to Equation (4). Even if the solvent guest does not bind very strongly to the host, a molecular displacement has to take place in order to develop the desired host–guest complex, and as our results demonstrate, the energetics of this displacement process can have a significant influence on the outcome of entropy calculations. Furthermore, the inclusion of one or more solvent molecules in the reactant structures is easily converted and should not increase the computational costs drastically.

Conclusion

In this study, we presented and compared the results of density functional calculations on large pseudorotaxane complexes and have compared these to experimental values based on NMR titrations. The results obtained from the geometry optimisation indicated the presence of three amide-type hydrogen bonds in each pseudorotaxane. All of these bonds could be classified according to their bond lengths, which were found to be similar for the w→a(1) and a→w bonds in all complexes. This is also true in the case of the elongated hydrogen bond w→a(2).

The calculated adiabatic interaction energies are very similar for **1–2** (MeO-) to **1–6** (NO_2-) and differ only by ~3 kJ mol^{-1}, whereas **1–7** (CH_2Cl_2) and **1–8** ($CHCl_3$) show significantly reduced interaction energies due to the smaller number and different types of hydrogen bonds. In contrast, the water-containing compounds **1–9** (H_2O) and **1–10** ($(H_2O)_4$) yield rather large values of around ~20 kJ mol^{-1} per hydrogen bond, which agree well with the hydrogen-bond energy of pure water.

The question of how rotaxanes can be modified is answered by the following observations. Our results indicate that the overall intermolecular interaction is affected only slightly by the functional groups at the axle's end. However, the isolated axle's dipole moment shows a strong dependence on the functional ending group. An increase in dipole moment was observed with the trend of a reduced absolute interaction energy, indicating that the hydrogen bonds work as a steric hindrance for the ideal total dipole arrangement. All hydrogen-bond strengths obtained from the SEN method agree well with the interatomic distances of the optimised geometries in predicting two strong and one weak hydrogen bond for each pseudorotaxane. The stability trend obtained from the supramolecular approach is quite properly reproduced by the SEN method as well. As the most important results, the SEN analysis reveals opposite trends for the individual hydrogen bonds: The proton-donating bridges a→w decrease from **1–2** (MeO-) to **1–6** (NO_2-), whereas both proton-accepting bridges increase from **1–2** (MeO-) to **1–6** (NO_2-). This explains why in total almost no trend is observed. For a closer inspection of substituent effects, we thus recommend the examination of guests featuring only a single hydrogen-bond function, as in the case of the truncated structures illustrated in Figure 2. The interaction energies

obtained for these systems show a pronounced substituent effect (see Table 4). This is in accordance with Chang et al., who observed similar trends for the proton-donating bridge from the macrocycle.[32]

For the thermochemical analysis we proposed two different models, namely the direct formation according to Equation (4) and the guest-exchange reaction formulated in Equation (5). Comparison of the thermochemical quantities obtained from both models shows a significant influence of the entropic contribution, which differs by about $\sim 45\,kJ\,mol^{-1}$ at 298 K. As a consequence, only the exchange-reaction path could predict stable pseudorotaxane complexes and thus was chosen as the variant closer to the experiment. A mixed approach considering interaction energies from COSMO calculations and thermal corrections from pure gas-phase calculations resulted in stable pseudorotaxanes according to the exchange mechanism [Eq. (5)] as well, but predicted free reaction enthalpies with absolute values being about $22\,kJ\,mol^{-1}$ lower than the original values. Upon comparison with the experimental values obtained from NMR titrations, we find good agreement between theory and experiment for all investigated complexes.

Thus, the guest-exchange reaction path might be an appropriate ansatz for the static quantum chemical calculation of thermochemical properties in supramolecular architectures, which partly covers the influence of the solvent by including one or more solvent molecules as supramolecular guests to the first-principles calculation. In the case of the amide-type pseudorotaxanes **1–2** to **1–6**, the experimental free reaction enthalpies are accurately reproduced by the explicit treatment and the corresponding exchange reaction.

Acknowledgement

We acknowledge the financial support of the DFG priority program SPP 1191 "Ionic Liquids" and the ERA project "A Modular Approach to Multi-responsive Surfactant/Peptide (SP) and Surfactant/Peptide/Nanoparticle (SPN) Hybrid Materials". We would also like to acknowledge the financial support from the collaborative research center SFB 624 "Templates" at the University of Bonn. Special acknowledgements go to Professor M. Reiher, ETH Zürich, and Professor F. Neese, University of Bonn, for the generous allocation of computational resources.

[1] C. A. Schalley, T. Weilandt, J. Brüggemann, F. Vögtle, *Top. Curr. Chem.* **2004**, *248*, 141.
[2] V. Balzani, A. Credi, S. Silvi, M. Venturi, *Chem. Soc. Rev.* **2006**, *35*, 1135.
[3] C. A. Schalley, K. Beizai, F. Vögtle, *Acc. Chem. Res.* **2001**, *34*, 465.
[4] D. A. Leigh, A. Troisi, F. Zerbetto, *Angew. Chem.* **2000**, *112*, 358; *Angew. Chem. Int. Ed.* **2000**, *39*, 350.
[5] M. J. Blanco, M. C. Jiménez, J. C. Chambron, V. Heitz, M. Linke, J. P. Sauvage, *Chem. Soc. Rev.* **1999**, *28*, 293.
[6] P. D. Boyer, *Angew. Chem.* **1998**, *110*, 2424; *Angew. Chem. Int. Ed.* **1998**, *37*, 2297.
[7] J. E. Walker, *Angew. Chem.* **1998**, *110*, 2438; *Angew. Chem. Int. Ed.* **1998**, *37*, 2309.
[8] W. R. Browne, B. L. Feringa, *Nat. Nanotechnol.* **2006**, *1*, 25.
[9] "Theoretical Methods for Supramolecular Chemistry", B. Kirchner, M. Reiher in *Analytical Methods in Supramolecular Chemistry* (Ed.: C. A. Schalley), Wiley-VCH, Weinheim, **2007**.
[10] X. Zheng, K. Sohlberg, *J. Phys. Chem. A* **2006**, *110*, 11862.
[11] E. Marand, Q. Hu, H. W. Gibson, B. Veytsman, *Macromolecules* **1996**, *29*, 2555.
[12] C. A. Schalley, W. Reckien, S. D. Peyerimhoff, B. Baytekin, F. Vögtle, *Chem. Eur. J.* **2004**, *10*, 4777.
[13] F. Vögtle, T. Dünnwald, T. Schmidt, *Acc. Chem. Res.* **1996**, *29*, 451.
[14] W. Reckien, S. D. Peyerimhoff, *J. Phys. Chem. A* **2003**, *107*, 9634.
[15] W. Reckien, B. Kirchner, S. D Peyerimhoff, *J. Phys. Chem. A* **2006**, *110*, 12963.
[16] R. Castro, M. J. Berardi, E. Córdova, M. O. de Olza, A. E. Kaifer, J. D. Evanseck, *J. Am. Chem. Soc.* **1996**, *118*, 10257.
[17] Y. H. Jang, S. Hwang, Y. Kim, S. S. Jang, W. A. Goddard III, *J. Am. Chem. Soc.* **2004**, *126*, 12636.
[18] W. Deng, R. P. Muller, W. A. Goddard III, *J. Am. Chem. Soc.* **2004**, *126*, 13562.
[19] W. Reckien, private communication.
[20] D. H. Busch, N. A. Stephensen, *Coord. Chem. Rev.* **1990**, *100*, 119.
[21] R. Cacciapaglia, L. Mandolini, *Chem. Soc. Rev.* **1993**, *22*, 221.
[22] N. V. Gerbeleu, V. B. Arion, J. Burgess, *Template Synthesis of Macrocyclic Compounds*, Wiley-VCH, Weinheim, **1999**.
[23] *Templated Organic Synthesis* (Eds.: F. Diederich, P. Stang), Wiley-VCH, Weinheim, **2000**.
[24] T. J. Hubin, D. H. Busch, *Coord. Chem. Rev.* **2000**, *200*, 5.
[25] J. P. Sauvage, *Acc. Chem. Res.* **1990**, *23*, 319.
[26] J. C. Chambron, C. O. Dietrich-Buchecker, V. Heitz, J. F. Nierengarten, J. P. Sauvage, C. Pascard, J. Guilhem, *Pure Appl. Chem.* **1995**, *67*, 233.
[27] *Molecular Catenanes, Rotaxanes, and Knots* (Eds.: J. P. Sauvage, C. Dietrich-Buchecker), Wiley-VCH, Weinheim, **1999**.
[28] D. Amabilino, J. F. Stoddart, *Chem. Rev.* **1995**, *95*, 2725.
[29] P. T. Glink, J. F. Stoddart, *Pure Appl. Chem.* **1998**, *70*, 419.
[30] S. A. Nepogodiev, J. F. Stoddart, *Chem. Rev.* **1998**, *98*, 1959.
[31] C. Seel, A. H. Parham, O. Safarowsky, G. M. Hubner, F. Vögtle, *J. Org. Chem.* **1999**, *64*, 7236.
[32] S. Y. Chang, H. S. Kim, K. J. Chang, K. S. Jeong, *Org. Lett.* **2004**, *6*, 181.
[33] C. A. Hunter, *J. Chem. Soc. Chem. Commun.* **1991**, 749.
[34] C. A. Hunter, *J. Am. Chem. Soc.* **1992**, *114*, 5303.
[35] F. Vögtle, S. Meier, R. Hoss, *Angew. Chem.* **1992**, *104*, 1628; *Angew. Chem. Int. Ed. Engl.* **1992**, *31*, 1619.
[36] U. F. Röhrig, L. Guidoni, U. Röthlisberger, *ChemPhysChem* **2005**, *6*, 1836.
[37] A. R. Jacobsen, A. N. Markis, L. M. Sayre, *J. Org. Chem.* **1987**, *52*, 2592.
[38] J. Druzian, C. Zucco, M. C. Rezendre, F. Nome, *J. Org. Chem.* **1989**, *54*, 4767.
[39] T. Ziegler, *Sci. Synth.* **2005**, *21*, 43.
[40] K. A. Connors, *Binding Constants*, Wiley, New York, **1987**.
[41] "Determination of binding constants", K. Hirose in *Analytical Methods in Supramolecular Chemistry* (Ed.: C. A. Schalley), Wiley-VCH, Weinheim, **2007**.
[42] H. Gampp, M. Maeder, C. J. Meyer, A. D. Zuberbühler, *Talanta* **1986**, *33*, 943.
[43] K. Eichkorn, O. Treutler, H. Öhm, M. Häeser, R. Ahlrichs, *Chem. Phys. Lett.* **1995**, *240*, 283.
[44] A. Schäfer, C. Huber, R. Ahlrichs, *J. Chem. Phys.* **1994**, *100*, 5829.
[45] A. D. Becke, *Phys. Rev. A* **1988**, *38*, 3098.
[46] R. Ahlrichs, M. Bär, M. Häser, H. Horn, C. Kölmel, *Chem. Phys. Lett.* **1989**, *162*, 165.
[47] S. F. Boys, F. Bernardi, *Mol. Phys.* **1970**, *19*, 553.
[48] B. Kirchner, *J. Chem. Phys.* **2005**, *123*, 204116.
[49] S. Koßmann, J. Thar, P. A. Hunt, T. Welton, B. Kirchner, *J. Chem. Phys.* **2006**, *124*, 174506.
[50] S. Kristyán, P. Pulay, *Chem. Phys. Lett.* **1994**, *229*, 175.
[51] P. Hobza, J. Šponer, T. Reschel, *J. Comput. Chem.* **1995**, *16*, 1315.
[52] E. R. Davidson, *J. Chem. Phys.* **1967**, *46*, 3320.

[53] K. R. Roby, *Mol. Phys.* **1974**, *27*, 81.
[54] M. Reiher, D. Sellmann, B. Hess, *Theor. Chem. Acc.* **2001**, *106*, 379.
[55] B. Kirchner, M. Reiher, *J. Am. Chem. Soc.* **2005**, *127*, 8785.
[56] M. Reiher, B. Kirchner, *J. Phys. Chem. A* **2003**, *107*, 4141.
[57] J. Thar, B. Kirchner, *J. Phys. Chem. A* **2006**, *110*, 4229.
[58] W. Reckien, M. Eggers, F. Vögtle, C. A. Schalley, S. D. Peyerimhoff, B. Kirchner, to be published.
[59] J. Neugebauer, M. Reiher, C. Kind, B. A. Hess, *J. Comput. Chem.* **2002**, *23*, 895.
[60] D. A. McQuarrie, J. D. Simon, *Physical Chemistry*, University Science Books, Sausalito, **1997**.
[61] A. Schäfer, A. Klamt, D. Sattel, J. Lohrenz, F. Eckert, *Phys. Chem. Chem. Phys.* **2000**, *2*, 2187.
[62] T. Hupp, C. Sturm, E. M. B. Janke, M. P. Cabre, K. Weisz, B. Engels, *J. Phys. Chem. A* **2005**, *109*, 1703.
[63] S. Schlund, C. Schmuck, B. Engels, *J. Am. Chem. Soc.* **2005**, *127*, 11115.
[64] A. J. Doig, D. H. Williams, *J. Am. Chem. Soc.* **1992**, *114*, 338.
[65] Gaussian 03, Revision C.02, M. J. Frisch, G. W. Trucks, H. B. Schlegel, G. E. Scuseria, M. A. Robb, J. R. Cheeseman, J. A. Montgomery, Jr., T. Vreven, K. N. Kudin, J. C. Burant, J. M. Millam, S. S. Iyengar, J. Tomasi, V. Barone, B. Mennucci, M. Cossi, G. Scalmani, N. Rega, G. A. Petersson, H. Nakatsuji, M. Hada, M. Ehara, K. Toyota, R. Fukuda, J. Hasegawa, M. Ishida, T. Nakajima, Y. Honda, O. Kitao, H. Nakai, M. Klene, X. Li, J. E. Knox, H. P. Hratchian, J. B. Cross, V. Bakken, C. Adamo, J. Jaramillo, R. Gomperts, R. E. Stratmann, O. Yazyev, A. J. Austin, R. Cammi, C. Pomelli, J. W. Ochterski, P. Y. Ayala, K. Morokuma, G. A. Voth, P. Salvador, J. J. Dannenberg, V. G. Zakrzewski, S. Dapprich, A. D. Daniels, M. C. Strain, O. Farkas, D. K. Malick, A. D. Rabuck, K. Raghavachari, J. B. Foresman, J. V. Ortiz, J. C. Burant, S. Clifford, P. Y. Ayala, Q. Cui, A. G. Baboul, S. Clifford, J. Cioslowski, B. B. Stefanov, G. Liu, A. Liashenko, P. Piskorz, I. Komaromi, R. L. Martin, D. J. Fox, T. Keith, M. A. Al-Laham, C. Y. Peng, A. Nanayakkara, M. Challacombe, P. M. W. Gill, B. Johnson, W. Chen, M. W. Wong, C. Gonzalez, J. A. Pople, Gaussian, Inc., Wallingford CT, **2004**.
[66] J. S. Binkley, J. A. Pople, W. J. Hehre, *J. Am. Chem. Soc.* **1980**, *102*, 939.
[67] M. S. Gordon, J. S. Binkley, J. A. Pople, W. J. Pietro, W. J. Hehre, *J. Am. Chem. Soc.* **1982**, *104*, 2797.
[68] R. Paulini, K. Müller, F. Diederich, *Angew. Chem.* **2005**, *117*, 1820; *Angew. Chem. Int. Ed.* **2005**, *44*, 1788.
[69] A. E. Reed, L. A. Curtiss, F. Weinhold, *Chem. Rev.* **1988**, *88*, 899.
[70] P. Carloni, U. Röthlisberger, M. Parrinello, *Acc. Chem. Res.* **2002**, *35*, 455.
[71] M. C. Colombo, L. Guidoni, A. Laio, A. Magistrato, P. Maurer, S. Piana, U. Röhrig, K. Spiegel, M. Sulpizi, J. V. Vondele, M. Zumstein, U. Röthlisberger, *Chimia* **2002**, *56*, 13.

Received: March 27, 2007
Revised: October 5, 2007
Published online: November 21, 2007

